POTENTIAL STRUCTURAL MATERIALS AND DESIGN CONCEPTS FOR LIGHT AIRPLANES, PART II

L. Pazmany, H. Prentice, C. Waterman, and F. Tietge
San Diego, California, U.S.A.

INTRODUCTION

This four-part paper is based on a study conducted by San Diego Aircraft Engineering Company for NASA, Mission Analysis Division, Ames Research Center. The complete report of the study was published as NASA CR-1285, March 1969; a summary report was published as NASA CR-73257.

The series of papers presented here contains material of possible interest to sailplane designers and builders. The NASA report CR-1285 is available for sale through CFSTI, Springfield, Virginia 22151.

Part I was presented in Technical Soaring, Vol. I, No. 4, April 1972. The remaining two parts of the paper will appear serially in forthcoming editions of this publication.

PART II

EVALUATION OF PROMISING CANDIDATE MATERIALS

The promising candidates are now compared on the basis of types of members and concepts. Composites, which are anisotropic, require some mention being made as to allowables versus fiber orientation. When these materials, in single-laminate configuration, are loaded at an angle to the direction of the fibers, their strength is reduced considerably. The reduction in allowable is a function of the angle. Figure 2 illustrates the effect due to the low shear transfer capability of the resin matrix. For this reason, composite systems are normally found in various combinations of fiber-oriented layers. As an example, a wing skin panel carrying torsion might require three layers with the following orientation (see Fig. 1):

Layers (1) and (3) stabilize the panel against shear buckling, while layer (2) resists the direct shear and axial loading in the panel skin. Figure 2 also shows variation in strength with several combinations of fiber orientations. Figure 3 indicates variation in compression modulus with change of filament direction. Basic good design practices, when using laminated structure, are presented in Fig. 4. Fiber-to-resin matrix proportion is another important relationship, strength-wise. A resin-rich composite is weakened by the influence of the lower strength matrix, while a resin-starved composite is unsatisfactory because of insufficient bonding between each fiber. In filament-wound structures, 70-to-85 percent by volume is considered normal for fiber

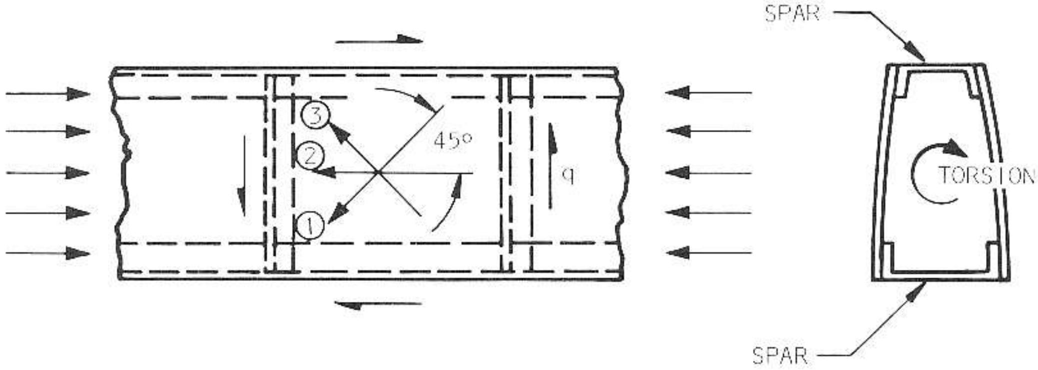

FIGURE 1

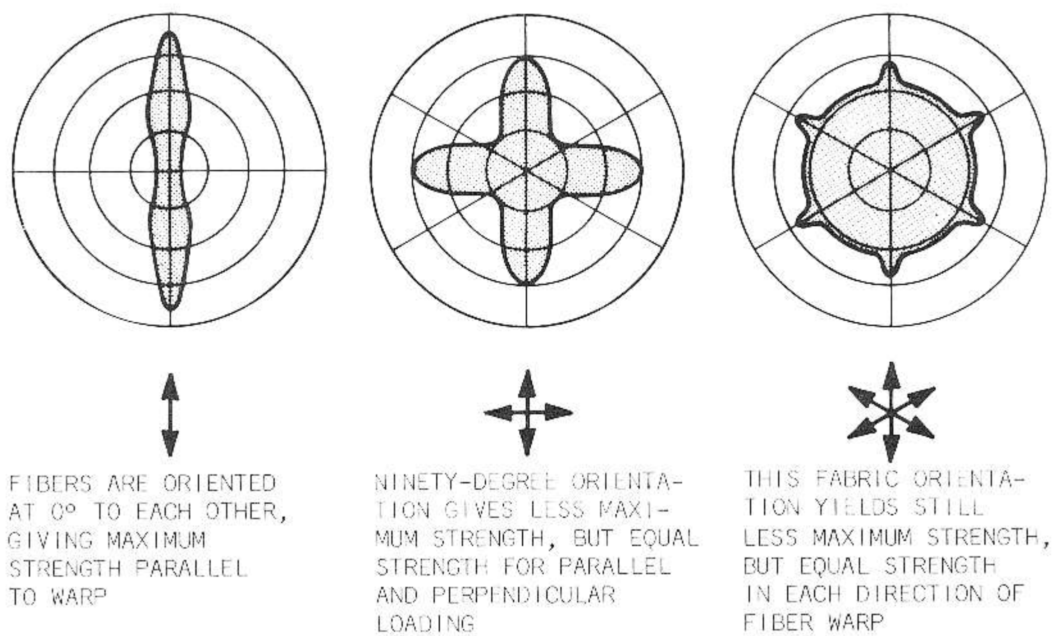

FIGURE 2

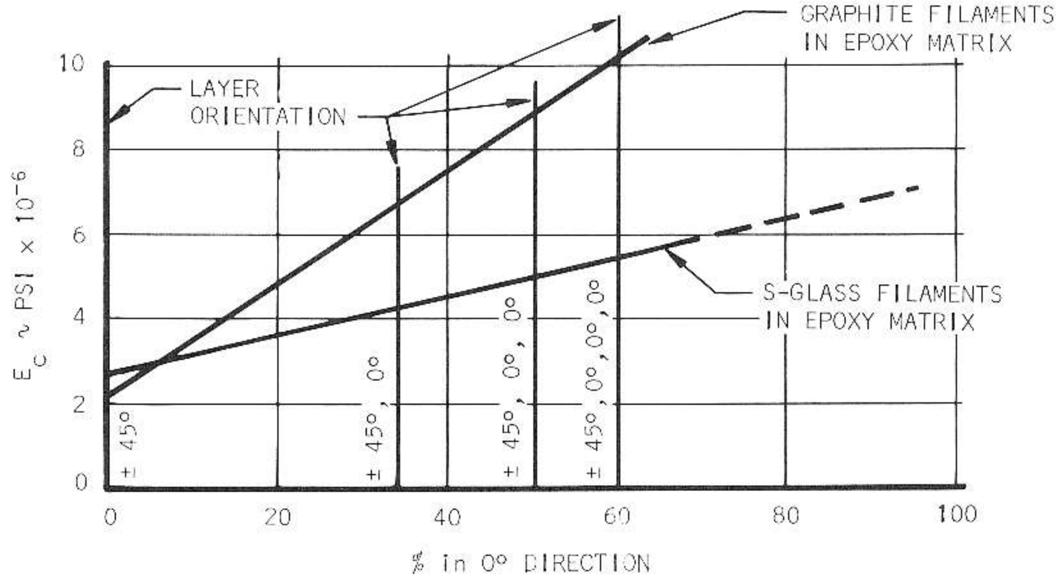

FIGURE 3

content. Included in the comparisons, where appropriate, are several composite laminate combinations. A summary of the basic properties of candidates is presented in Table I. For more detailed or added information, see Ref. 1.

Tension Members

Fig. 6 shows weight per inch versus axial load (4,000 pounds maximum) for the various materials. The ordinate provides for the use of an efficiency factor which might be encountered under conditions of riveting or welding.

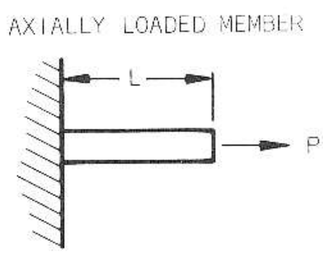

FIGURE 5

Derivations: $f = \frac{P}{A}$, $W = A\ L\ w$,

$A = \frac{W}{L\ w}$ and $f = K_{eff}\ F$

To develop curves of $\frac{WK}{L}$ efficiency versus Tension Load P , let:

$$K_{eff}\ F = \frac{P}{W/L\ w}$$

$$K_{eff}\ \frac{W}{L} = \frac{P}{F/w} \quad \text{(Fig. 6)}$$

Symbols:

f	= Stress
A	= Cross-section area
W	= Weight
w	= Density
K_{eff}	= Efficiency factor
F	= Smaller of F_{tu} or: $1.5\ F_{ty}$

Simple Columns (assume round tubes)

Structural indexes were used to assist in the evaluation of promising candidate materials when applied as simple columns. As defined in Ref. 4, a structural index is a measure of loading

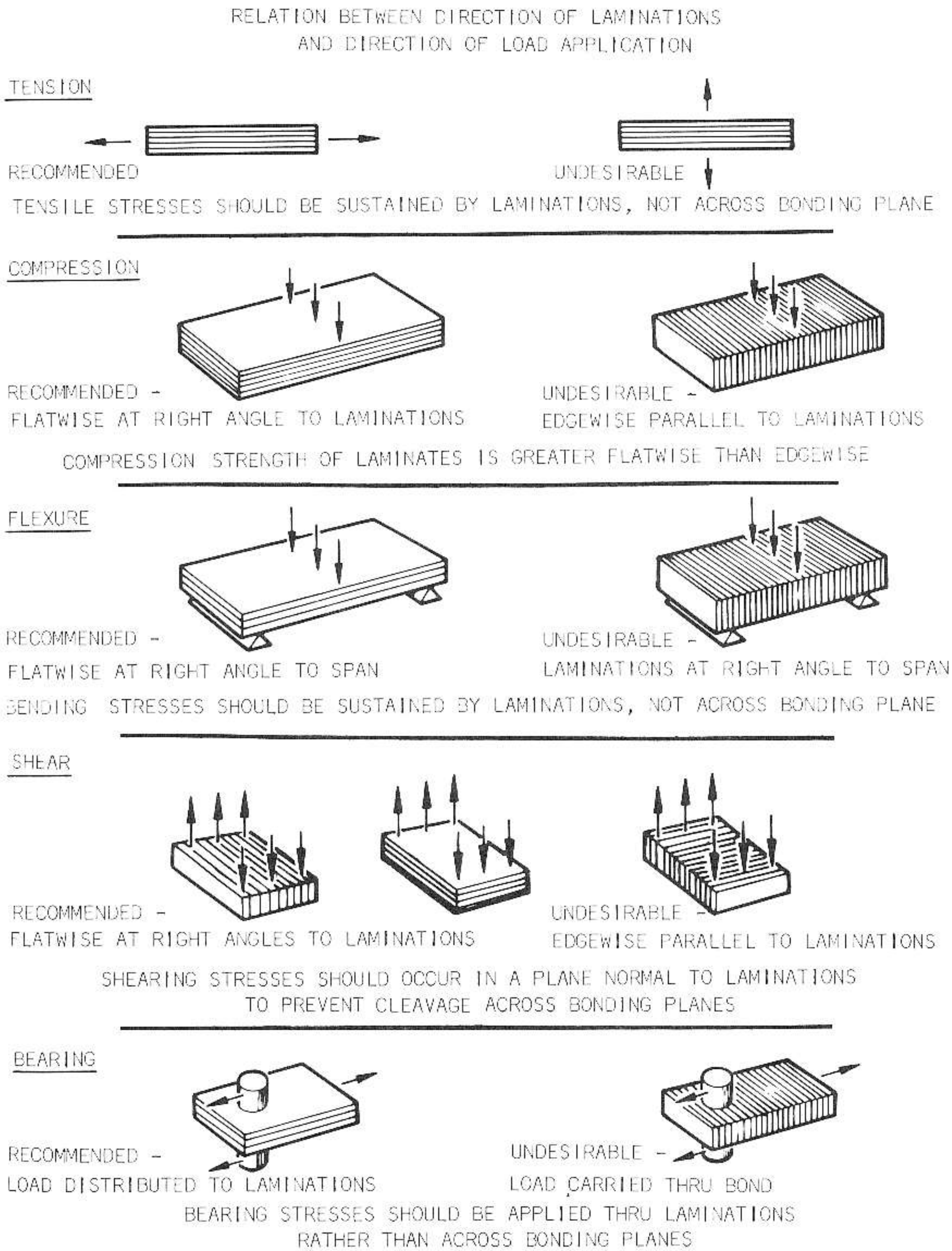
RELATION BETWEEN DIRECTION OF LAMINATIONS
AND DIRECTION OF LOAD APPLICATION
TENSION
RECOMMENDED
UNDESIRABLE
TENSILE STRESSES SHOULD BE SUSTAINED BY LAMINATIONS, NOT ACROSS BONDING PLANE
COMPRESSION
RECOMMENDED -
FLATWISE AT RIGHT ANGLE TO LAMINATIONS
UNDESIRABLE -
EDGEWISE PARALLEL TO LAMINATIONS
COMPRESSION STRENGTH OF LAMINATES IS GREATER FLATWISE THAN EDGEWISE
FLEXURE
RECOMMENDED -
FLATWISE AT RIGHT ANGLE TO SPAN
UNDESIRABLE -
LAMINATIONS AT RIGHT ANGLE TO SPAN
BENDING STRESSES SHOULD BE SUSTAINED BY LAMINATIONS, NOT ACROSS BONDING PLANE
SHEAR
RECOMMENDED -
FLATWISE AT RIGHT ANGLES TO LAMINATIONS
UNDESIRABLE -
EDGEWISE PARALLEL TO LAMINATIONS
SHEARING STRESSES SHOULD OCCUR IN A PLANE NORMAL TO LAMINATIONS
TO PREVENT CLEAVAGE ACROSS BONDING PLANES
BEARING
RECOMMENDED -
LOAD DISTRIBUTED TO LAMINATIONS
UNDESIRABLE -
LOAD CARRIED THRU BOND
BEARING STRESSES SHOULD BE APPLIED THRU LAMINATIONS
RATHER THAN ACROSS BONDING PLANES

FIGURE 4

TABLE I. PROMISING CANDIDATE MATERIALS--NON-METALLIC

MATERIAL	APPLI-CATION	F_{tu}	F_{ty}	F_{cu}	F_{su}	E_c	e	w	WEATHER-ABILITY	MATERIAL COST ②	THERMAL CO-EFF. $\alpha/10^5$	COMPARATIVE STRUCTURAL EFFICIENCIES $\frac{F_{tu}}{w}$	$\frac{F_{tu}}{w\ \$/LB}$	$\frac{\sqrt{E_c}}{w}$	$\frac{\sqrt{E_c}}{w\ \$/LB}$	$\frac{\sqrt[3]{E_c}}{w}$	$\frac{\sqrt[3]{E_c}}{w\ \$/LB}$	REF
	③	KSI	KSI	KSI	KSI	$\frac{PSI}{10^6}$	%	LB/IN^3		\$ / LB	in/in/°F							
NON-REINFORCED																		
ABS (High Strength)	NT-FT	7.3	-	10.4	-	.180	20	.039	EXCEL	0.46	6.00	187	407	11	24	14	31	5,21
NON-CONTINUOUS FIBER REINFORCED																		
3/8 E-Glass/Nylon 6/10	FT	20	-	18	11	1.0	5-6	.048	EXCEL	1.34 (0.65)	2.50	418	(645)	21	(32)	21	(32)	13
1" S-Glass/Epoxy	FT	45	-	62	8	7.8	-	.060	EXCEL	4.00 (2.00)	-	750	(375)	46	(23)	33	(16)	14
E-Glass/Polyester	NT	20	-	26	-	1.99	-	.070	EXCEL	0.63	1.20	286	454	20	32	15	29	12
CLOTH REINFORCED																		
DAP Prepreg	NT-FT	49 ①	-	-	-	2.6 ①	-	.070 ①	EXCEL	3.15 (1.58)	-	700	(446)	23	(14)	20	(12)	17,18
181 Cloth/E-Glass	NT-FT	45	-	45	-	3.3	-	.070	EXCEL	(1.00)	-	643	(643)	26	(26)	21	(21)	15
181 Cloth/S-Glass	NT-FT	94	-	65	-	4.2	-	.070	EXCEL	(2.00)	-	1340	(670)	29	(14)	23	(12)	16
FILAMENT REINFORCED (EPOXY MATRIX)																		
Unidirectional																		
Graphite	FT	95.9	-	56.5	5.2	15.4	-	.051	EXCEL	(1.00)	-	1870	(1870)	77	(77)	49	(49)	19
S-Glass	FT	210	-	120	13.6	7.6	-	.073	EXCEL	(2.00)	-	2880	(1440)	38	(19)	27	(13)	19
±45° Layers (t=.016 in)																		
Graphite	FT	5.8	-	31.6	24.8	2.1	-	.051	EXCEL	(1.00)	-	114	(114)	28	(28)	25	(25)	19
S-Glass	FT	17.7	-	37.3	50.0	2.5	-	.073	EXCEL	(2.00)	-	349	(174)	22	(11)	19	(10)	19
±45°,0° Layers (t=.024 in)																		
Graphite	FT	35.8	-	39.9	20.4	6.6	-	.051	EXCEL	(1.00)	-	702	(702)	50	(50)	37	(37)	19
S-Glass	FT	81.8	-	64.9	39.5	4.2	-	.073	EXCEL	(2.00)	-	1120	(560)	28	(14)	22	(11)	19
±45°,0°,0° Layers (t=.032 in)																		
Graphite	FT	50.8	-	44.0	17.8	8.8	-	.051	EXCEL	(1.00)	-	1000	(1000)	58	(58)	41	(20)	19
S-Glass	FT	113.8	-	78.7	34.0	5.1	-	.073	EXCEL	(2.00)	-	1560	(780)	31	(15)	24	(12)	19
±45°,0°,0°,0° Layers (t=.040 in)																		
Graphite	FT	59.8	-	46.5	15.9	10.2	-	.051	EXCEL	(1.00)	-	1170	(1170)	63	(63)	45	(45)	19
S-Glass	FT	133.1	-	86.9	30.5	5.6	-	.073	EXCEL	(2.00)	-	1825	(912)	32	(76)	24	(12)	19
WOOD				F_{cy}														
Sitka Spruce	NT	9.4	5.3	3.5	1.0	1.4	-	.015	POOR	0.67	-	626	935	79	118	-	-	24
Mahogany/Poplar Plywd	NT	6.7	-	2.6	1.9	.9	-	.020	POOR	7.05	-	335	167	48	23	48	23	24
Spruce - Staypak	NT	35.8	25.9	4.3	1.3	4.7	.75	.047	FAIR	④	-	760	④	46	④	-	-	24

NOTES: ① ESTIMATED ② ( ) = 1982 ESTIMATE ③ NT - NEAR TERM, FT - FAR TERM ④ EXPERIMENTAL, NO PRICE AVAILABLE

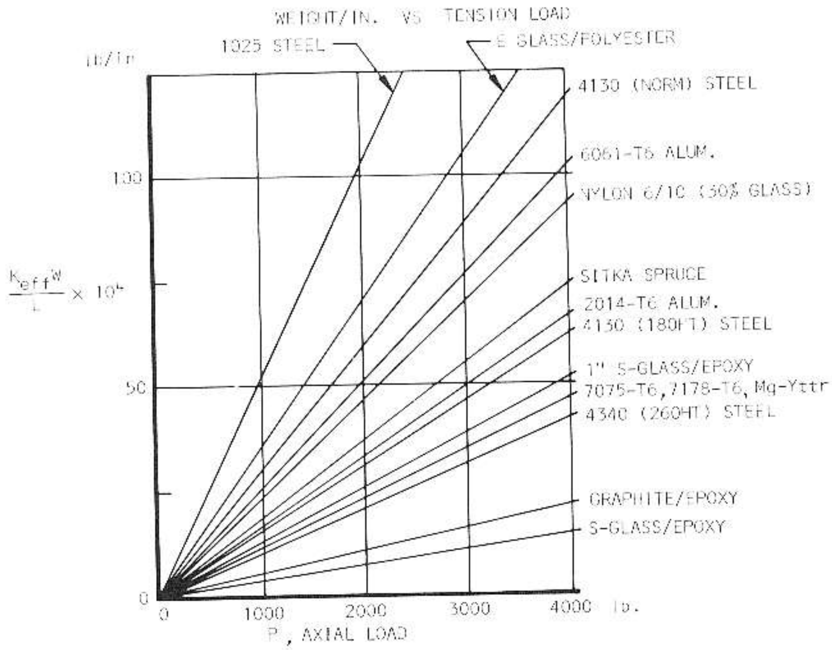

FIGURE 6

intensity and has the advantage of eliminating the effect of size in dealing with allowable stresses. For a simple column, the structural index becomes P/L^2. Derivations:

Primary buckling $$F_c = \pi\left(\sqrt{E_t}\right)\left(\sqrt{\frac{D}{8rt}}\right)\left(\sqrt{\frac{P}{L^2}}\right)$$

and crippling $$F_{cr} = K_2 \frac{\sqrt{EE_t}}{D/t}$$

Equating the two equations gives optimum value of D/t:

$$\left(D/t\right)_{opt} = 2\left(\frac{K_2^2 \quad E}{\pi P/L^2}\right)^{1/3} =$$

$$0.742 \left(\frac{E}{P/L^2}\right)^{1/3}$$

$$\left[K_2 = 0.40 \text{ (Ref. 4)}\right]$$

Fig. 7 plots D/t ratios versus structural index for the materials under consideration.

Compression Structure

Probably the most detailed and extensive evaluation of structure occurs during the design of compression critical sections of the airframe. The section under compression is generally treated either as a wide column or a compression panel. The wide-column approach is used when the length of the panel is short compared to its width, as in a multi-rib wing box. A compression panel concept is assumed when the length of the panel is long compared to its width, as in a multi-spar wing box. To obtain allowable compression stresses for optimum round tube columns, substitute the value for optimum D/t in the primary buckling equation:

$$P/L^2 = \frac{8f^3}{\pi K_2 E^{1/2} E_t^{\ 3/2}} = \frac{6.37\ f^3}{E^{1/2} E_t^{\ 3/2}}$$

For study purposes, limit f to $0.80F_{cy}$

The allowable F_c may then be calculated and plotted for various materials, as shown in Fig. 8.

It is now possible to develop a formula for minimum weight, as follows:

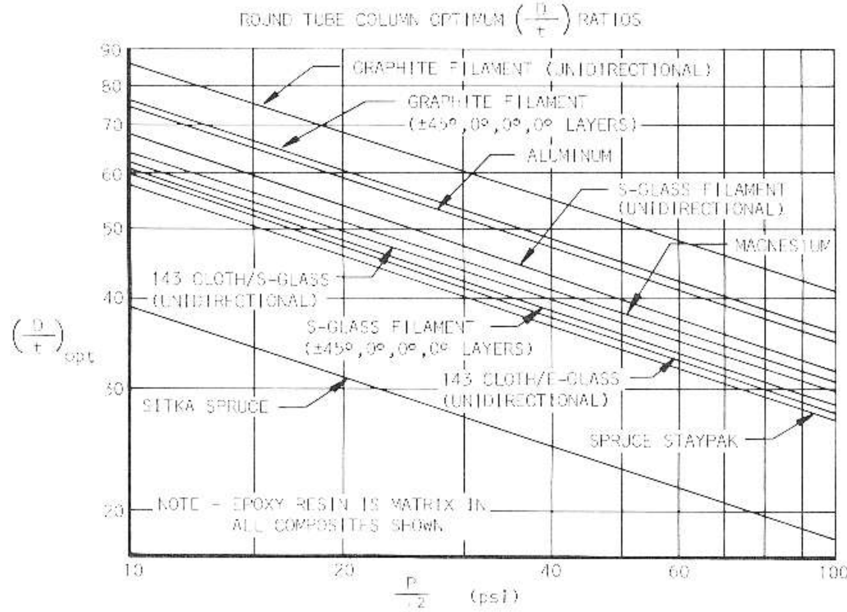

FIGURE 7

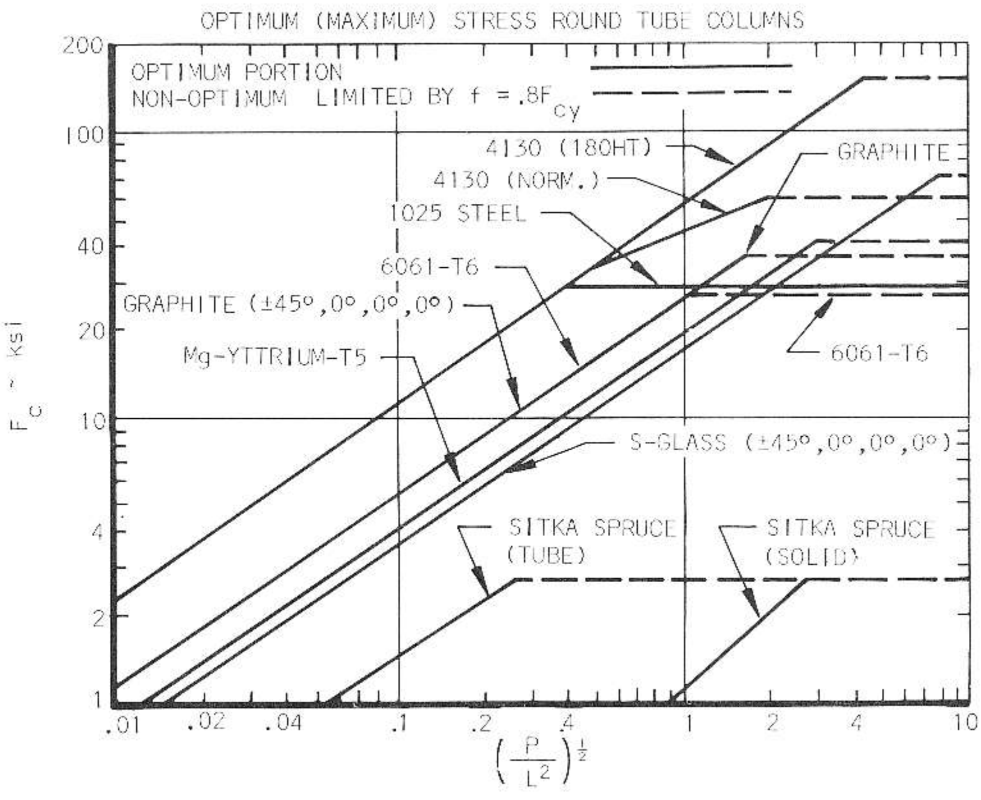

FIGURE 8

(1) Divide structural index by allowable F_c and multiply by density of material:

$$\frac{P\,(w)\,/L^2}{F_c}$$

(2) By substituting $\frac{P}{F_c} = A$ & $w = \frac{W}{AL}$, the following identity is obtained: $WC/L^3 = \frac{P/L^2}{F_{c/w}}$,

where C is restraint coefficient.

Values for WC/L^3 versus P/L^2 may now be determined and plotted for a number of materials (see Fig. 9).

The wide-column analysis assumes primary buckling between the ribs, which provide simple supports for loaded edges of the column. The following equation, taken from Ref. 5, is a result of equating general and local instability formulas:

$$\frac{N_x}{L\bar{\eta}E} = \epsilon\left(\bar{t}/L\right)^2$$ Where:

N_x = compressive load in pound/inch

L = length of column in inches

$\bar{\eta}$ = plasticity reduction factor

E = modulus of elasticity. psi

$\bar{t}$ = cross-sectional area per unit width

ϵ = efficiency factor, a function of buckling coefficient & shape factor

The analysis of compression panels is based upon all edges of the panel being simply supported, while plate theory expressions for local and general stability are equated to obtain the following equation:

$$\frac{N_x}{b\bar{\eta}E} = \epsilon\left(\bar{t}/b\right)^n$$ Where:

b = width of plate

n = an exponent which is a function of configuration

In the evaluation of wide-column and compression panel concepts, truss core sandwich, honeycomb sandwich, flat plate, and zee-stiffened plate construction will be considered for each case.

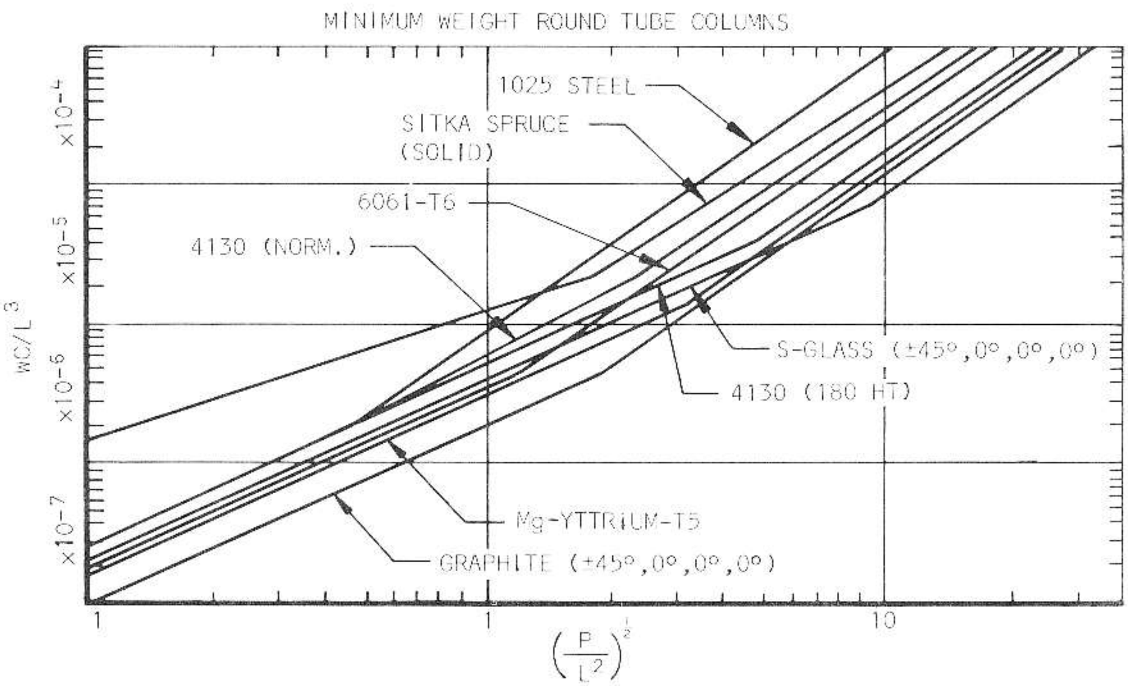

FIGURE 9

Minimum area equations for optimized wide columns and compression panels of zee-stiffened plate, flat plate, and truss coré sandwich construction are presented in Table II. Efficiency factors, ϵ, were obtained from Ref. 5, while the plasticity reduction factor, $\overline{\eta}$, was taken as unity for all cases.

Minimum area curves for truss core sandwich, honeycomb sandwich, flat plate, and zee-stiffened plate of wide column and compression panel construction are shown in Fig. 10 and Fig. 11.

The zee-stiffened plate, flat plate, and truss core curves were developed from the data in Table II. Minimum area curves for honeycomb sandwich were obtained from Ref. 5. Curves were generated by calculating typical weights and strengths, and algebraically converting the results to the general form of the other configurations. As stated in Ref. 5, the high efficiency of honeycomb sandwich construction is attributed to the fact that the full compressive strength of face sheets can be utilized by reducing the cell size of the honeycomb core.

A panel optimization computer program was used in Ref. 3 for evaluating numerous filament-wound materials in truss core and honeycomb sandwich construction. These configurations, in their optimum proportions of unidirectional to cross-ply fibers, are pictured in Fig. 12. By utilizing data from Ref. 3, optimum weight and corresponding core thickness versus structural index may be determined for graphite and S-Glass wide columns and compression panels.

Resulting values are plotted in Figs. 13 thru Fig. 15. Optimized configuration weights reflect $\pm 45^{0}$ fiber orientation in the skins for the most efficient alignment to react torsional shear. Minimum skin gages are set at 0.020 inches. Four failure modes considered were: general buckling, face wrinkling, intercell buckling, and shear crimping.

Minimum weight diagrams can also be developed from minimum area curves in Fig. 10 and Fig. 11, as follows:

(1) Multiply ordinate $\overline{t}/L$ by material density, w:

$w\overline{t}/L = W/bL^2$ because $W = bL\overline{t}w$,

$w = W/bL\overline{t}$

(2) Multiply abscissa N_x/LE by material modulus, E:

$EN_x/LE = N_x/L$; the weight is thus presented as a function of the structural index: N_x/L (or q/L).

Minimum weights for various materials and concepts are shown in Fig. 17 and Fig. 18.

In the discussion of sheet stringer-type wide columns, mention should be made of extruded Y stringers developed by NACA (NACA TN 1389) for increasing allowable stresses in compression structures. Figure 19 compares allowable stress versus structural index of sheet stringer wide columns constructed of 2024 and 7075 Y-stringers against a 2024 conventional stringer envelope.

These same constructions are compared on a weight basis in Fig. 20 which was derived from optimum stress curves by dividing N_x/L by F_c and then multiplying by w to obtain:

$$\left(N_x/L\right)\left(1/F_c\right)\left(w\right) = \overline{t}w/L = W/bL^2$$

Shear Panels

Wing, fuselage, and empennage skins on small aircraft (including helicopters) are of light-gage construction. Loading intensities due to torsional shear are low level; therefore, the panels are normally designed for shear buckling at the 1-to-1.2 g level. This requirement is established for appearance purposes, since the panel itself has ample strength to carry the ultimate torsional shear flow as a tension field member.

Materials for shear panel application are compared on a thickness basis in Fig. 21. The curves were obtained through a substitution and division process of the shear buckling equation for flat plates.

TABLE II

MINIMUM AREA EQUATIONS FOR OPTIMIZED WIDE COLUMNS AND COMPRESSION PANELS (Reference 28)

TYPE OF CONSTRUCTION	WIDE COLUMN	COMPRESSION PANEL
Zee-Stiffened Plate	$\frac{N_x}{LE} = 0.911\ (\bar{t}/L)^2$	$\frac{N_x}{bE} = 1.030\ (\bar{t}/b)^{2.36}$
Truss Core Sandwich	$\frac{N_x}{LE} = 0.605\ (\bar{t}/L)^2$	$\frac{N_x}{bE} = 1.108\ (\bar{t}/b)^2$
Flat (unstiffened) Plate	$\frac{N_x}{LE} = 0.823\ (\bar{t}/L)^3$	$\frac{N_x}{bE} = 3.62\ (\bar{t}/b)^3$

MINIMUM AREA CURVES - WIDE COLUMN CONCEPT

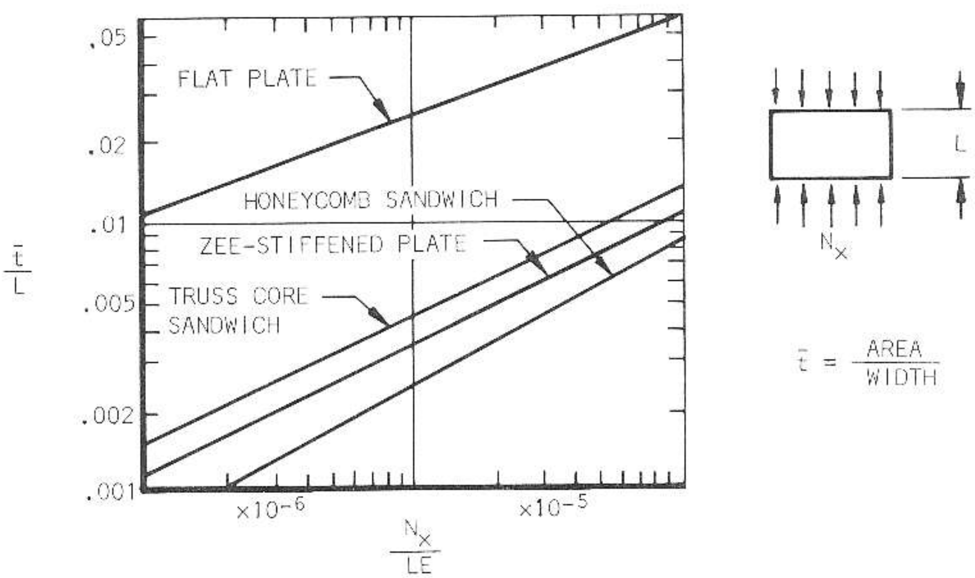

FIGURE 10

MINIMUM AREA CURVES - COMPRESSION PANEL CONCEPT

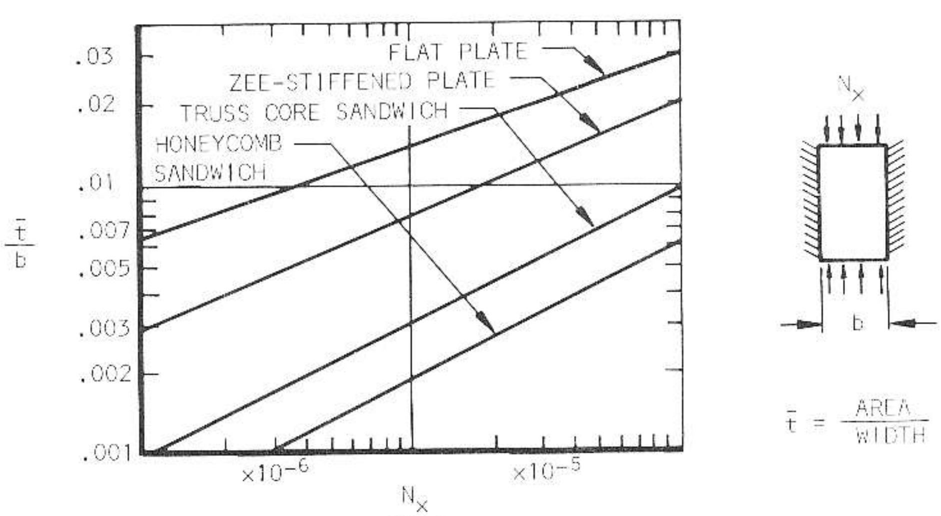

FIGURE 11

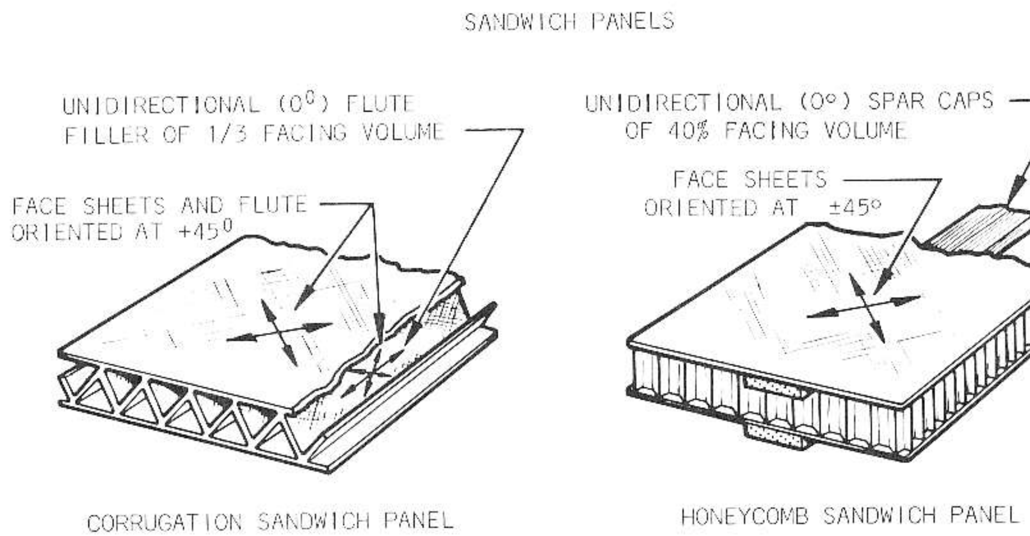

FIGURE 12

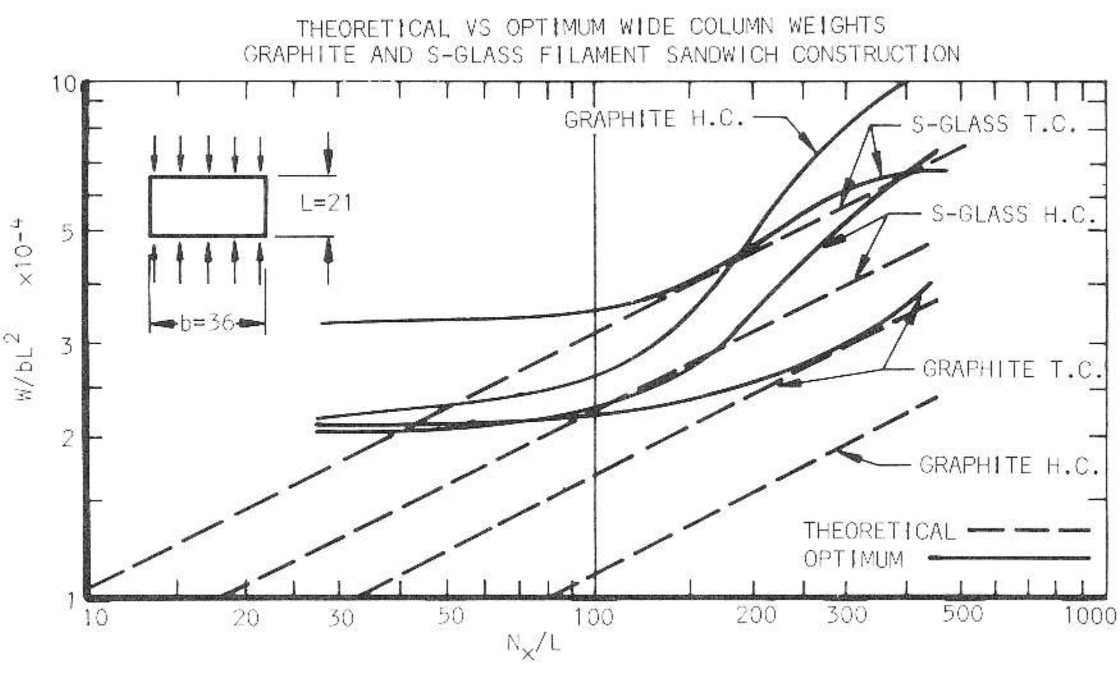

FIGURE 13

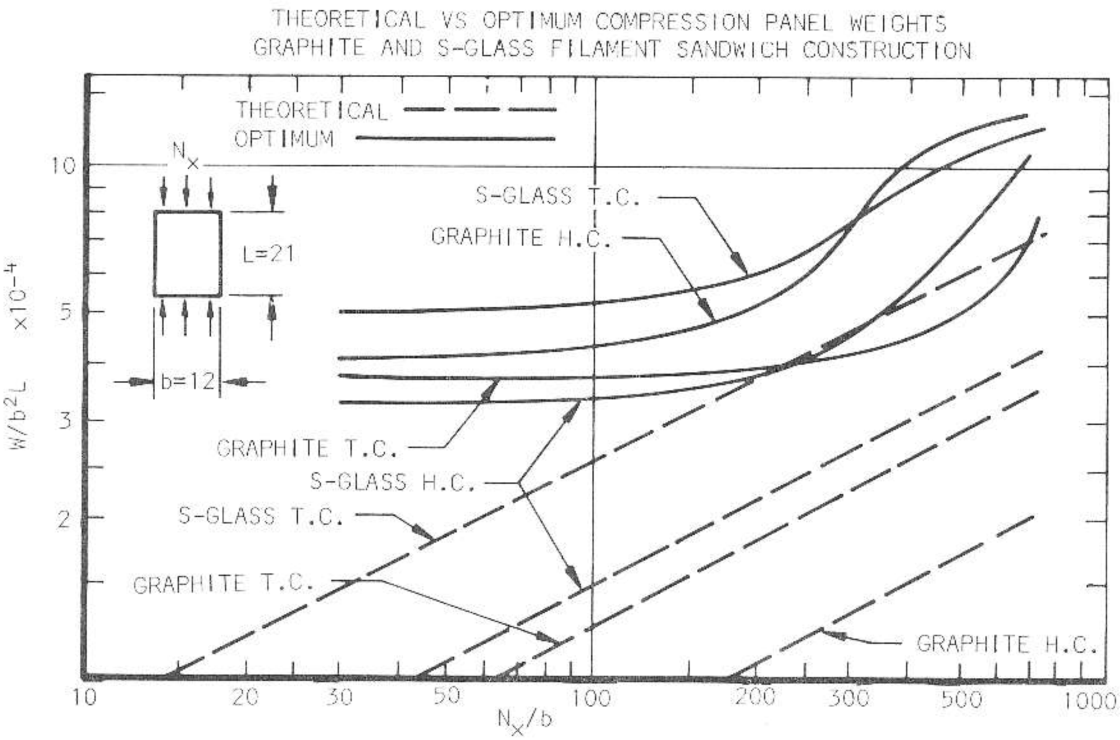

FIGURE 14

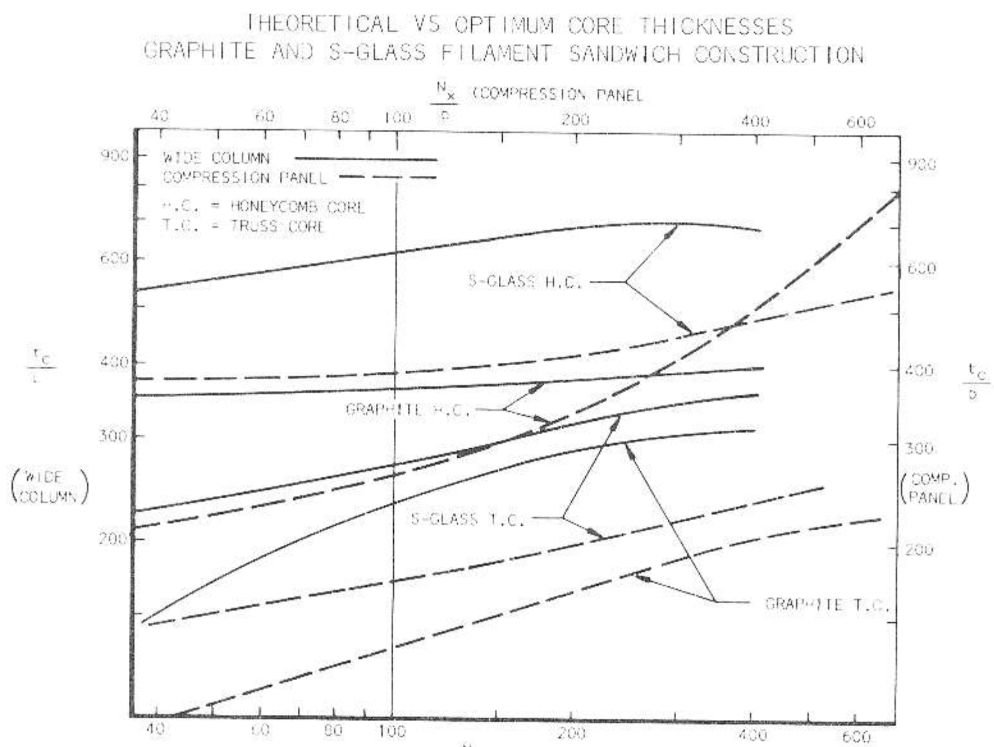

FIGURE 15

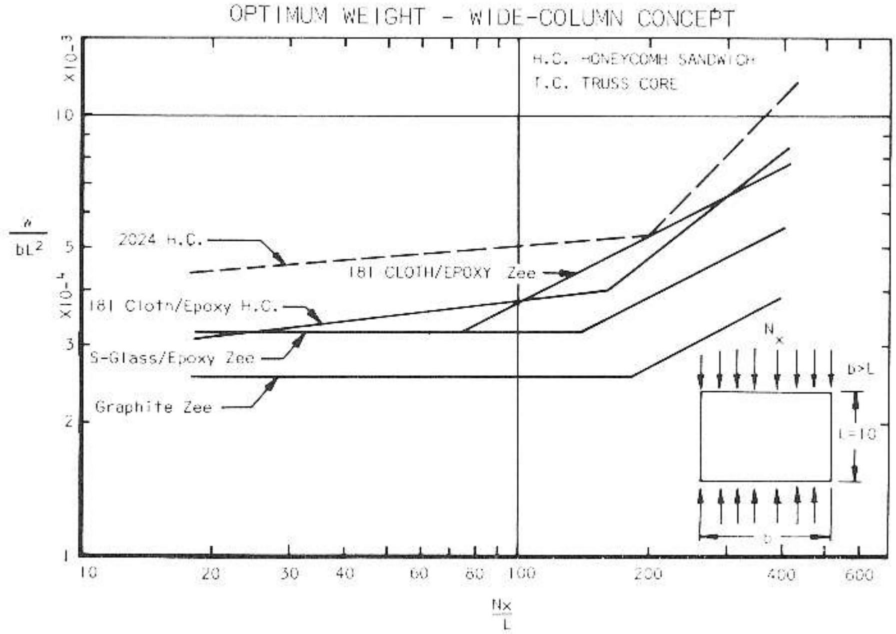

FIGURE 16

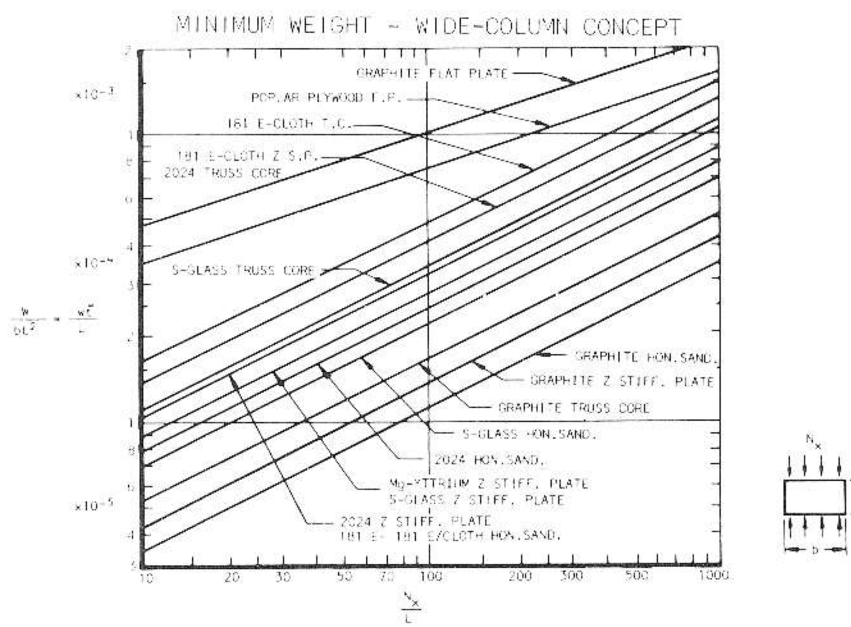

FIGURE 17

MINIMUM WEIGHT - COMPRESSION PANEL CONCEPT

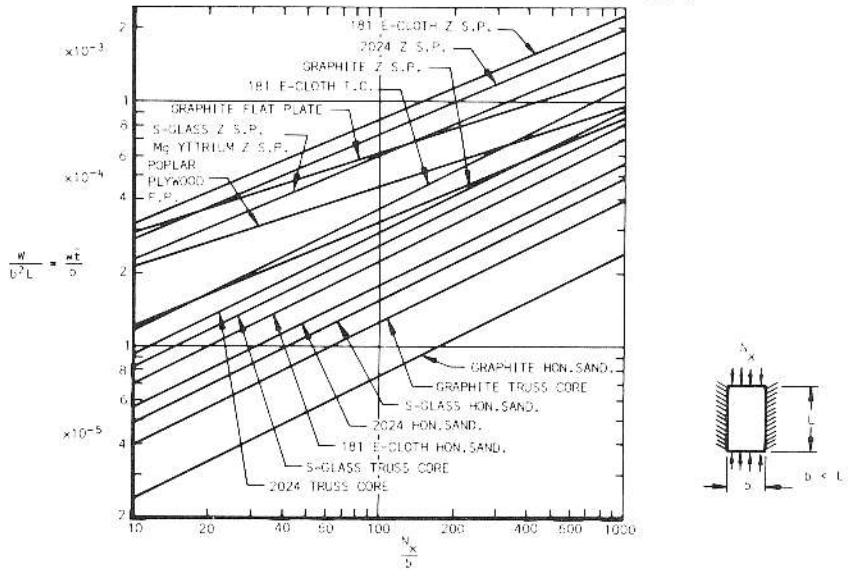

S.P. = STIFFENED PLATE
F.P. = FLAT PLATE

H.C. = HONEYCOMB SANDWICH = HONEYCOMB CORE
T.C. = TRUSS CORE

FIGURE 18

OPTIMUM (MAX.) STRESS - WIDE COLUMNS
ALUMINUM SHEET - STRINGER TYPE

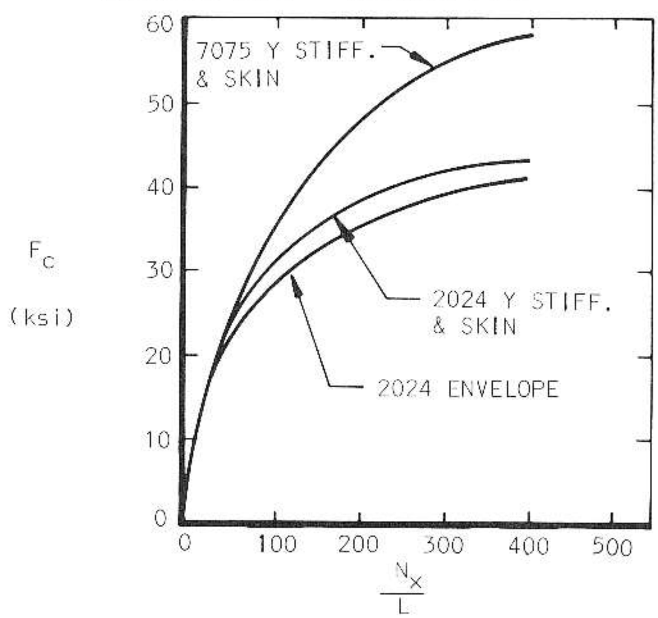

FIGURE 19

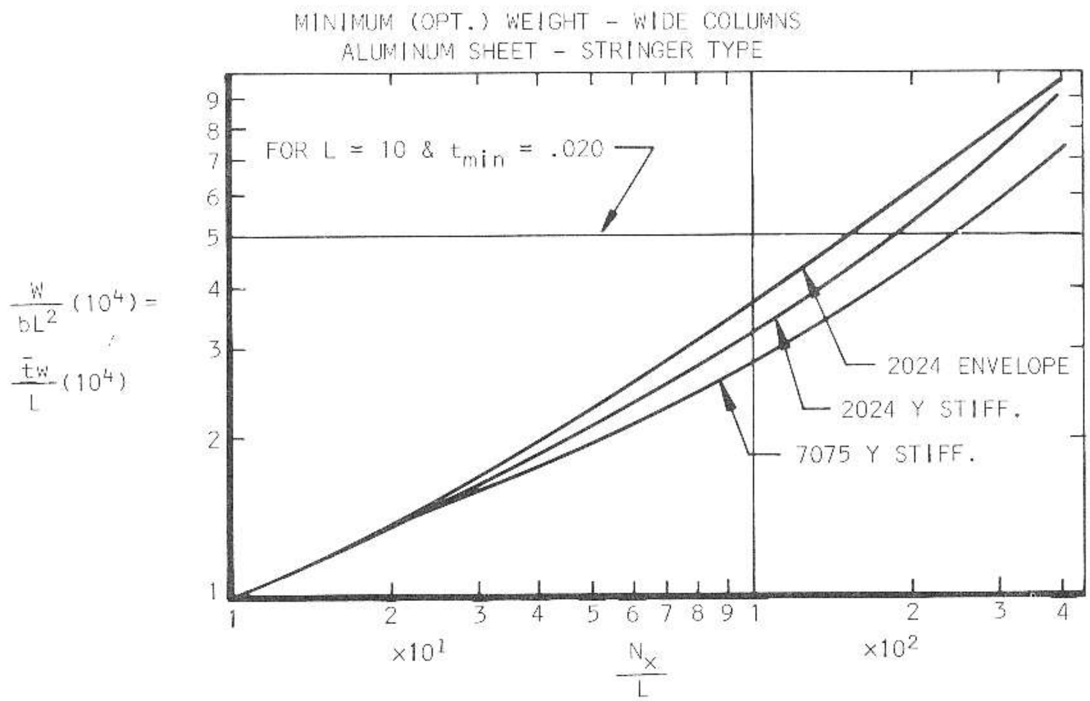

FIGURE 20

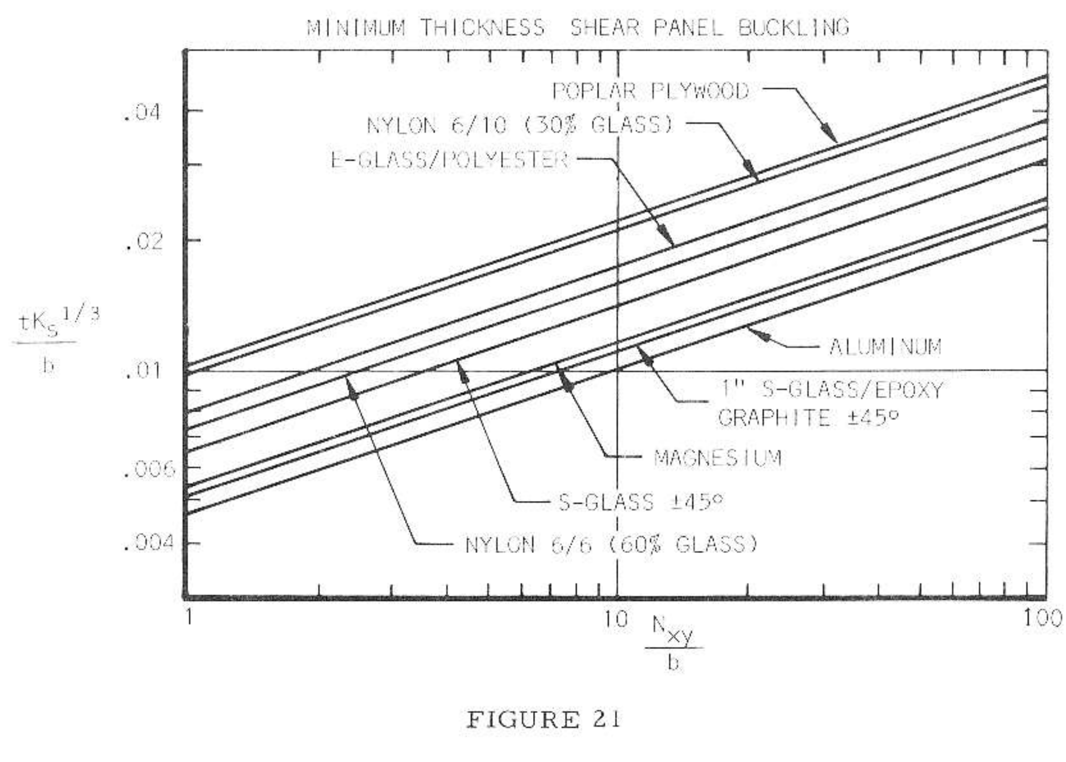

FIGURE 21

Shear buckling: $\tau_{cr} = \dfrac{K_s E_c t^2}{b^2}$

$\tau_{cr} = N_{xy}/t$,

$N_{xy} = q$ = torsional shear flow;

Where:

τ_{cr} = shear stress at which panel will buckle

K_s = shear buckling coefficient dependent upon edge conditions around panel (see Fig. 22)

b = short side dimension of panel

t = panel thickness

E_c = compression modulus of elasticity

Therefore:

$$N_{xy}/t = \frac{K_s E_c t^2}{b^2}, \quad N_{xy} = \frac{K_s E_c t^3}{b^2}$$

Obtain structural index (abscissa):

$$N_{xy}/b = \frac{K_s E_c t^3}{b^3} = K_s E_c (t/b)^3$$

Calculate ordinate:

$$t/b \;\sqrt[3]{K_s} = (N_{xy}/bE)^{1/3}$$

Minimum weights versus structural indexes for flat plate shear panel materials are presented in Fig. 23. Curves were derived by multiplying shear buckling equations, as modified for minimum thickness form, by material density, w:

$$wt/b \;\sqrt[3]{K_s} = w\,(Nxy/bE)^{1/3}$$

But: $W = wabt$, $w = W/abt$

Where: W = panel weight
a = long side of panel

Therefore:

$$W/b^2a = \sqrt[3]{K_s} = w\,(N_{xy}/bE)^{1/3}$$

Shear buckling coefficients, K_s , for various edge conditions are shown in Fig. 21.

Compression Flanges

In reviewing candidate materials for use as compression flanges on spars and similar bending members, the following structural index will be applied to represent crippling efficiency:

$$S = \frac{\sqrt{F_{cy} E_c}}{w}$$

This relationship is in general agreement with Needham's equation for crippling in Ref. 6 and assumes b/t, flange width to thickness ratio, to remain constant.

Crippling structural efficiencies for candidate materials are illustrated in Fig. 24. (References on p. 42).

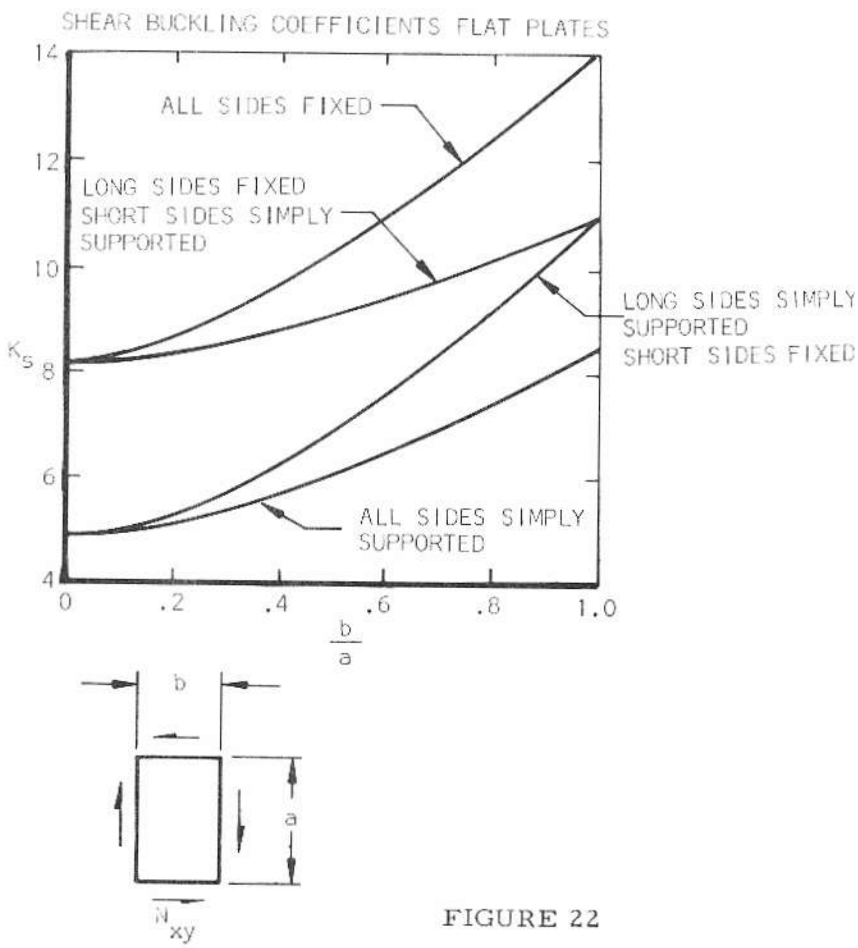

FIGURE 22

U.S. Air Force, Air Force Manual 51-9, Aircraft Performance, U.S. Government Printing Office, March 25, 1968.

U.S. Air Force, Air Force Manual 51-40, Vol. I, Air Navigation, U.S. Government Printing Office, August 1, 1968.

U.S. Naval Oceanographic Office, H. O. Pub. No. 216, Air Navigation, U.S. Government Printing Office, 1967.

U.S. Navy, Aerodynamics for Naval Aviators, NAVWEPS 00-80T-80, U.S. Government Printing Office, 1960.

MARYNIAK REFERENCES CONTINUED FROM P. 3

8. K. Petrikat and E. Pieruschka, "Die Stabilitätsbedingungen des Fieseler Deichselschepps," Jahrbuch, 1942, Deutschen Luftfahrtforschung.

9. J. Sandauer, Obciażenia sztywnego szybowca w locie holowanym w burzliwej atmosferze, Prace Instytutu Lotnictwa Warszawa Nr 43, 1970.

10. Modern Numerical Methods, Prepared by the National Physical Laboratory, Teddington, Middlesex, State Scientific and Technical Press, Warszawa, 1965.

PAZMANY REFERENCES -- FROM P. 23

REFERENCES

1. Anon.: MIL-HDBK-17, Plastics for Flight Vehicles (Part I, Reinforced Plastics).

2. Anon.: Application of Glass Fiber Laminates in Aircraft. AC 20-21, Federal Aviation Agency, 1964.

3. Whinery, D., North American Aviation, Inc.; Fernandez, D., Aerojet General Corporation: Manufacturing Methods for Plastic Airframe Structures By Filament Winding. Technical Report IR-9-371(V), August 1967. Air Force Materials Laboratory, WPAFB, Ohio.

4. Shanley, F. R.: Weight-Strength Analysis of Aircraft Structures. Dover Publications, Inc., New York, 1960.

5. Lyman, J.; Forest, J.; Porter, F.: Design and Analytical Study of Composite Structures. General Dynamics/Convair Division, Report GDC-ERR-AN-1077, Dec. 1966.

6. Bruhn, E. F.: Analysis and Design of Flight Vehicle Structures. Tri-State Offset Company, Cincinnati, Ohio, 1965.

END OF PART II

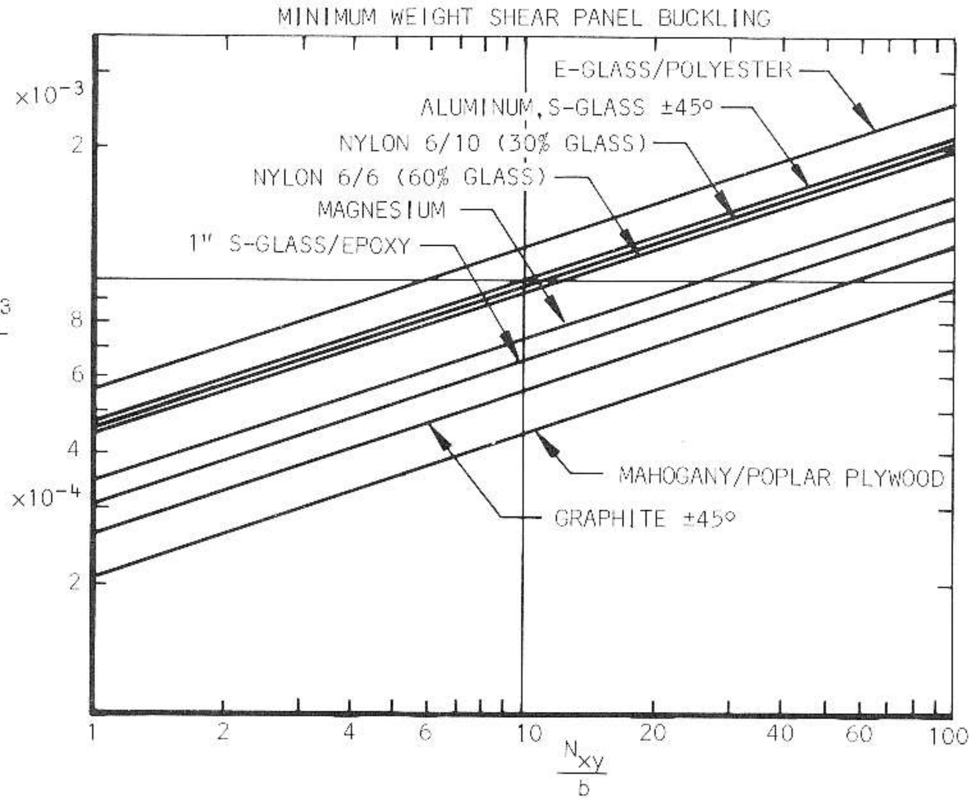

FIGURE 23

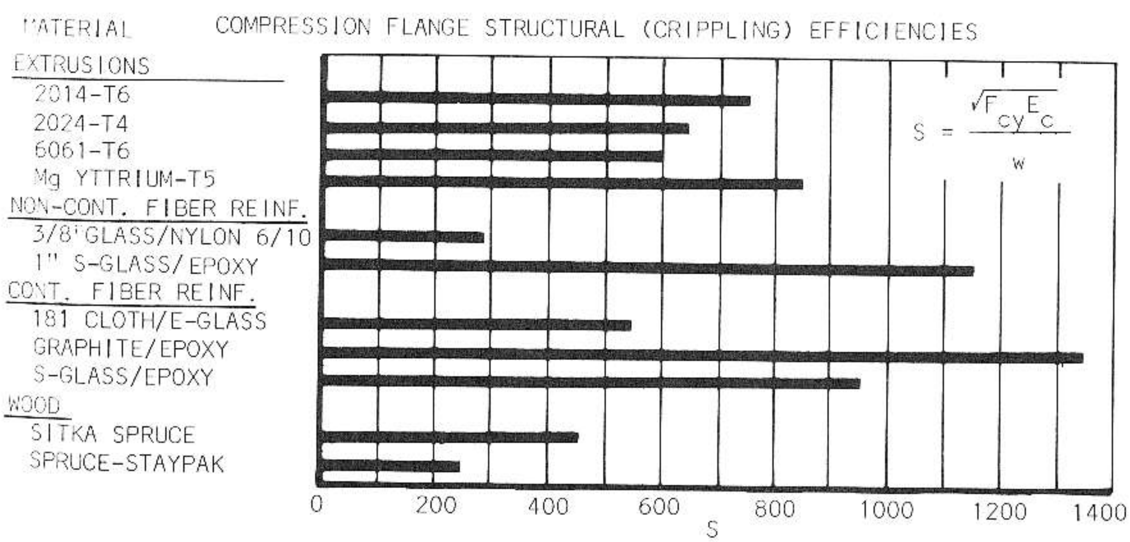

FIGURE 24